AIP | Advances

Optically tunable acoustic wave band-pass filter

N. Swinteck, P. Lucas, and P. A. Deymier

Citation: AIP Advances **4**, 124603 (2014); doi: 10.1063/1.4904075
View online: http://dx.doi.org/10.1063/1.4904075
View Table of Contents: http://scitation.aip.org/content/aip/journal/adva/4/12?ver=pdfcov
Published by the AIP Publishing

Optically tunable acoustic wave band-pass filter

N. Swinteck, P. Lucas, and P. A. Deymier
Department of Materials Science and Engineering, University of Arizona, Tucson, AZ 85721, USA

(Received 1 October 2014; accepted 2 December 2014; published online 9 December 2014)

The acoustic properties of a hybrid composite that exhibits both photonic and phononic behavior are investigated numerically with finite-element and finite-difference time-domain simulations. The structure is constituted of a periodic array of photonic resonant cavities embedded in a background superlattice. The resonant cavities contain a photo-elastic chalcogenide glass that undergoes atomic-scale structural reorganization when irradiated with light having energy close to its band-gap. Photo-excitation of the chalcogenide glass changes its elastic properties and, consequently, augments the acoustic transmission spectrum of the composite. By modulating the intensity of light irradiating the hybrid photonic/phononic structure, the position and spectral width of phonon passing-bands can be controlled. This demonstration offers the technological platform for optically-tunable acoustic wave band-pass filters. [http://dx.doi.org/10.1063/1.4904075]

I. INTRODUCTION

A phononic crystal (PC) is a composite structure comprised of a spatially periodic array of inclusions of one material embedded in a different background matrix material. PCs come in one-, two- and three-dimensional forms and, depending on their application, have length scales that vary from meters to several hundreds of nanometers. Phonon dispersion in PCs can be controlled by (1) varying the shape and/or filling fraction of the dispersed inclusions or (2) selecting alternative constituent materials with different elastic properties. In their history, phononic structures have been engineered with phonon dispersion curves showing frequency band-gaps (Bragg gaps) for longitudinal and shear waves[1–4] as well as passing bands with unique refractive properties such as negative refraction[5–11] and zero-angle refraction.[12–14] Several useful applications have been suggested from these spectral (ω-space) and wave vector (k-space) properties, such as (1) materials to isolate vibrations,[15,16] (2) composites to guide acoustic and elastic waves[17–21] and (3) devices to focus/collimate phonons.[22–24] Similar functionalities have been demonstrated for semi-infinite systems.[25] and PC plates.[26,27]

In spite of more than 20 years of research, PCs have found limited success in transitioning from the laboratory to industry. The primary reason resides in the fact that the advantage of using current PC technology in modern devices does not outweigh the detriment of replacing outright the technologies used presently in industry with comparable functions. The current state of knowledge and technical development in the field of phononics indicates a strong need for PCs with more diverse functionalities. Toward achieving this goal, some investigators have considered the efficacy of coupling linear waves to anharmonic modes in phononic systems employing nonlinear materials. This strategy, for instance, enabled theoretical[28] and experimental[29] demonstrations of acoustic rectification. Other investigators have considered controlling phonons in PCs with external stimuli such as an applied magnetic field.[30,31] In these works, exploitation of magnetoacoustic coupling led to PCs with tunable acoustic properties[30] and facilitated the development of reconfigurable phononic waveguides.[31]

Indeed these functionalities are unattainable in ordinary materials which gives tunable phononic systems a distinct advantage over other technologies for future industrial applications. With this as motivation, we aim to explore the scientific and technological merit of incorporating chalcogenide

glasses into phononic crystal designs. Chalcogenide glasses are a distinct class of amorphous semiconductors that exhibit a wide range of intriguing, light-induced phenomena such as photo-darkening,[32] photo-expansion,[33] photo-anisotropy[34] and photo-fluidity.[35] Moreover, some chalcogenide glasses exhibit photo-elasticity,[36] a phenomenon where the elastic properties of the glass change when irradiated with light having energy close to its band-gap. Utilizing a photo-elastic chalcogenide glass as a constituent material in a phononic structure is a pathway toward achieving novel acoustic functionalities as phonon dispersion depends on the electromagnetic radiation impinging upon the system.

In this work, we exploit the phenomenon of photo-elasticity in chalcogenide glasses to offer a tunable phononic material with acoustic properties dependent on the intensity of light irradiating the structure. A hybrid composite exhibiting both photonic and phononic properties is considered. The structure is constituted of a periodic array of photonic resonant cavities embedded in a background superlattice. The photonic resonant cavities contain a photo-elastic chalcogenide glass. When irradiated with light of a particular wavelength, a photonic eigenmode is activated inside the cavities which induces photo-elastic softening of the longitudinal elastic constant (C_{11}) of the chalcogenide glass. This strongly augments phonon dispersion and, consequently, the acoustic transmission spectrum of the superlattice. Due to the reversible nature of photo-elasticity in chalcogenide glasses,[36] when the light source is removed the acoustic properties of the superlattice are restored back to that of the non-irradiated system. This technology offers a platform on which optically-tunable acoustic wave band-pass filters can be developed. This paper is organized as follows. First, in *Section II: Background*, the phenomenon of photo-elasticity in chalcogenide glasses is briefly reviewed. Second, in *Section III: Models and Methods*, we describe the numerical models, namely finite-element (FE) and finite-difference time-domain (FDTD) simulations, used to characterize wave propagation in the hybrid photonic/phononic superlattice. Subsequently, in *Section IV: Results and Discussion*, phonon dispersion curves and transmission spectra are presented for the superlattice under different photon irradiation conditions. Finally, in *Section V: Conclusions*, we comment on the efficacy of the demonstrated technology for radio frequency signal processing applications. The work presented in this paper represents a strong push to broaden the range of functionalities associated with phononic systems.

II. BACKGROUND

Chalcogenide glasses are comprised of chains of divalent atoms (S, Se and Te) cross-linked with elements of higher covalent coordination such as Ge, As and Sb. The atomic constituents of these materials have similar electronegativity and consequently the glass structure is described as a network of covalent bonds.[37] Chalcogenide glasses are amorphous semiconductors with band gap energies around 1-2 eV.[38] A distinct property of chalcogenide glasses is their ability to undergo structural reorganization during photo-excitation with light having energy close to its band-gap. The excitation of localized electrons from the top of the band-gap creates electron-hole pairs that facilitate the creation of metastable defect configurations within the covalent network. This phenomenon leads to such effects as photo-darkening,[32] photo-expansion,[33] photo-anisotropy,[34] photo-fluidity[35] and photo-elasticity.[36] Gump *et al*. demonstrated experimentally that the Ge-Se family of chalcogenide glasses undergo reversible changes in their elastic properties when irradiated with focused light having energy close to the material's band-gap.[36] Specifically, when irradiated with a laser at 2mW power, C_{11} of a glass with composition $GeSe_4$ was reduced by approximately 5% with respect to C_{11} for the non-irradiated system. In ramping-up the power of the laser to a maximum of 6mW, C_{11} of $GeSe_4$ was shown to decrease by as much as 50%. The stiffness of the glass was fully recovered upon ramping-down the laser from 6mW to 2mW, indicating that photo-elasticity in Ge-Se systems is a reversible phenomenon.

In this manuscript, $GeSe_4$ is utilized as a functional component in a hybrid phononic/photonic superlattice. The distinctive response of this material to photon irradiation enables the function of tunable phonon passing-bands. Similar functionality was recently demonstrated experimentally for a solid/fluid PC constituted of an array of steel cylinders in a background polymer hydrogel matrix.[39] In that work, with application of a thermal stimulus (infrared light), changes in the effective elastic properties of the hydrogel as well as the lattice constant of the PC could be induced, thereby

augmenting the phonon band structure of the system. The steel/hydrogel PC was suggested as a tunable filter for ultrasonic waves. In contrast to this work, the present study considers a system that is entirely solid and suitable for radio frequency signal processing applications. Specific details are highlighted in the next section.

III. MODEL AND METHODS

In this work, we utilize both FE and FDTD methodologies to characterize the acoustic properties of our system of interest. Though either method could have been used exclusively, we employed both techniques for computational convenience. FE simulations are facilitated by the commercial software package COMSOL Multiphysics whereas the algorithms for FDTD simulations were developed in-house. FE simulations are used to calculate dispersion diagrams for the photonic and phononic components of the proposed hybrid photonic/phononic structure. FDTD simulations are utilized to simulate the propagation of broad-band acoustic wave packets through the hybrid composite to ascertain data pertaining to acoustic wave transmission. As is shown in subsequent data plots, the agreement between both methods is excellent.

The primitive unit cell (supercell) of the hybrid photonic/phononic structure considered in this manuscript is picture in Figure 1(a).

It has periodicity (a_2) and is constituted of a slab of $GeSe_4$ (the *photonic resonance cavity*) sandwiched in between two quarter-wave Bragg reflectors. Each Bragg reflector is a photonic superlattice of periodicity (a_1) and consists of alternating layers of $GeSe_4$ and epoxy. The thickness of the $GeSe_4$ and epoxy layers is $\lambda/4$ where λ is the wavelength of light required to initiate photo-elastic softening of $GeSe_4$. FE simulations are employed to generate the photonic band structure of the

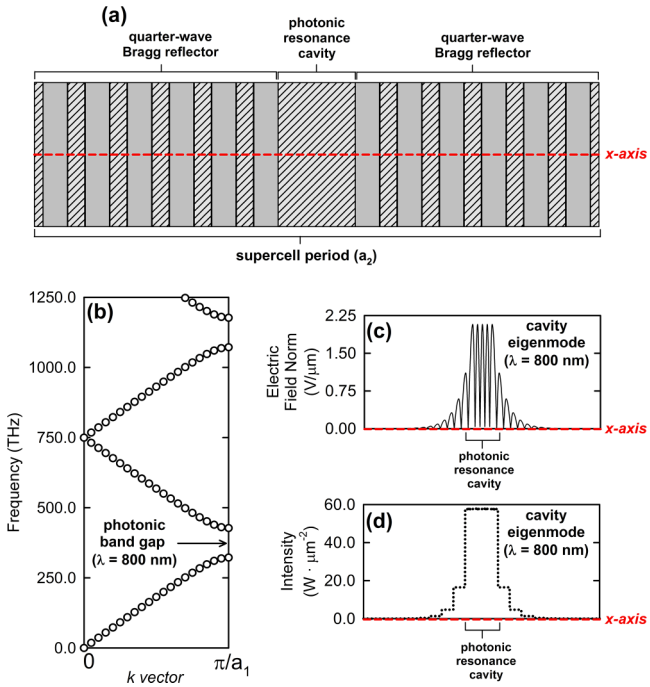

FIG. 1. (a) Illustration of supercell for the hybrid phononic/photonic superlattice. The supercell consists of a $GeSe_4$ slab (photonic resonance cavity) sandwiched in between two quarter-wave Bragg reflectors (photonic crystals) each comprised of alternating thin-films of $GeSe_4$ and epoxy resin. The characteristic length-scales of the quarter-wave Bragg stack and supercell are a_1 and a_2, respectively. Additionally, a_2 is the phononic lattice parameter. (b) Photonic band structure of an infinite quarter-wave Bragg reflector showing complete photonic band gap at irradiation wavelength (λ = 800 nm). (c) Horizontal cut along x-axis of the supercell showing normalized electric field for the cavity eigenmode at the irradiation wavelength (λ = 800 nm). Notice the strong localization on the $GeSe_4$ region of the structure. (d) same as (c) except for photon intensity.

Bragg reflectors with $n = 2.46$ and $n = 1.315$ for $GeSe_4$ and epoxy resin, respectively, where n is refractive index. These calculations indicate that the Bragg reflectors each possess a photonic band gap at $\lambda = 800$ nm (see Figure 1(b)). This, in combination with the fact that the photonic resonance cavity is λ thick, allows a photonic resonance mode to be established in the $GeSe_4$ cavity at the irradiation wavelength $\lambda = 800$ nm. Additional FE simulations are employed to characterize the normal modes supported in the $GeSe_4$ resonance cavity. Figures 1(c) and 1(d) show normalized electric field and photon intensity, respectively, along the *x-axis* of the superlattice for the cavity eigenmode at $\lambda = 800$ nm. Photon energy is strongly localized on the $GeSe_4$ region of the structure which induces large changes in the elastic properties of the material via the mechanism of photo-elasticity. The intensity associated with this eigenmode is not entirely confined within the bounds of the defect cavity. Accordingly, neighboring regions of $GeSe_4$ to the defect cavity will undergo photo-elastic softening as well. This detail is accounted for in subsequent FE and FDTD calculations involving the supercell.

In FE and FDTD simulations, $GeSe_4$ is modelled as an isotropic material with variable elastic properties that depend on light intensity. Two specific photon irradiation conditions are considered: *laser OFF* and *laser ON*. For the *OFF* condition, the structure is not irradiated with light. In this circumstance, the elastic properties of $GeSe_4$ are $\rho = 4361$ kg/m^3, $C_L = 2052$ m/s, $C_T = 1114$ m/s, where ρ is density, C_L is longitudinal speed of sound and C_T is transverse speed of sound.[40] For the *ON* condition, electromagnetic radiation impinges upon the hybrid photonic/phononic structure at power level equal to 6mW and excites photonic resonance modes compatible with the irradiation wavelength. This excitation coincides with significant photo-elastic softening of C_{11} of the chalcogenide glass. Accordingly, the elastic properties of $GeSe_4$ are modified under the assumption of 50% reduction in C_{11},[36] and 6.4% volume expansion to yield the following elastic properties: $\rho = 4099$ kg/m^3, $C_L = 1486$ m/s, $C_T = 578$ m/s. For epoxy resin, in both conditions, we use $\rho = 1180$ kg/m^3, $C_L = 2535$ m/s, $C_T = 1157$ m/s. The time-scale for photo-induced structural transition in Ge-Se chalcogenide glasses can be estimated from knowledge of the frequency interval over which Raman-active, vibrational modes reside. With typical values between 100 cm^{-1} - 500 cm^{-1},[37,38] the time-scale for transition between a stable covalent network of atoms to a metastable defect configuration via covalent bond switching is approximated to be on the order of several thousand atomic oscillations, or equivalently, a few hundred nanoseconds. This conservative estimate suggests that Ge-Se glasses can indeed be used as a platform for GHz-frequency filters capable of rapid-switching.

A finite system, comprised of 10 repetitions of the supercell pictured in Figure 1(a), is utilized for later FDTD simulations to compute phonon transmission spectra for the superlattice in the *laser OFF* and *laser ON* conditions. This configuration, sandwiched in between an inlet and outlet region of homogeneous $GeSe_4$, is illustrated in Figure 2.

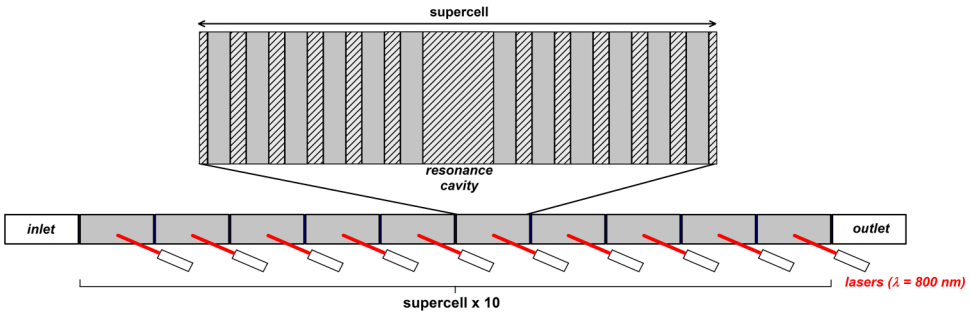

FIG. 2. Finite hybrid phononic/photonic superlattice comprised of 10 repetitions of the supercell pictured in Figure 1(a). This configuration is used for subsequent FDTD simulations to compute phonon transmission spectra for the superlattice in the *laser OFF* and *laser ON* conditions. Positioned above each supercell (resonance cavity) is a laser of wavelength λ. The structure is irradiated from the top at a grazing angle to maximize the longitudinal component of the light k-vector and ensure optimal coupling into the photonic resonance cavities.

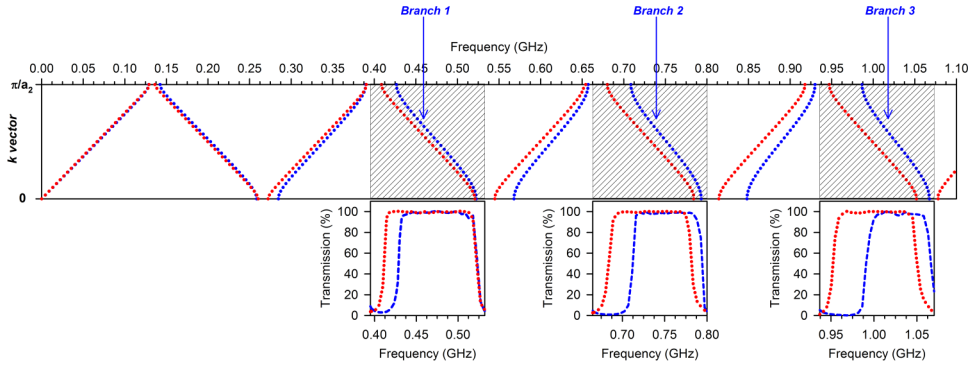

FIG. 3. (top) two superposed phonon dispersion curves for conditions of *laser OFF* (blue lines) and *laser ON* (red lines). Phonon band structures were computed with FE simulations (COMSOL Multiphysics). (bottom) three plots for phonon transmission corresponding to different phonon branches, *laser OFF* (blue lines) and *laser ON* (red lines). Photo-induced changes in the elastic properties of $GeSe_4$ facilitate active control over position and spectral width of phonon passing-bands.

In FDTD simulations, a broad-band pressure wave packet is launched from the inlet domain at normal incidence to the superlattice. The signal propagates through the finite hybrid phononic/photonic superlattice and exits the simulation at the end (right hand side) of the outlet domain. A probe in the outlet domain detects displacement over time, the Fourier transform of which provides insight on the spectral properties of the phononic system (e.g. acoustic band gaps and phonon passing-bands). In practice, Mur 1st order absorbing boundary conditions[41] are utilized to avoid reflections at the left and right ends of the simulation domain. In the following section we present results for the phononic properties of the superlattice under the irradiation conditions of *laser OFF* and *laser ON*.

IV. RESULTS AND DISCUSSION

In Figure 3 we show one plot (top) with two superposed phonon band structures and three plots (bottom) each with two superposed phonon transmission spectra for the hybrid superlattice when the lasers are *OFF* (blue lines) and *ON* (red lines).

The three phonon transmission plots zoom-in on specific regions of the phonon band structure to illuminate the change in position and spectral width of phonon passing-bands. When the structure is irradiated with monochromatic light (*laser ON*), phonon branches are down-shifted in frequency leading to substantial changes in the acoustic transmission properties of the overall structure. Specifically, the passing-bands identified in Figure 3 with markers *Branch 1*, *Branch 2* and *Branch 3* increase in width by 21.4%, 17.7% and 31.0%, respectively, when the lasers are turned on. Furthermore, the frequency values on which these bands are centered are modulated (down-shifted) by 1.2%, 2.3% and 3.1%, respectively. This example shows that an external light source can be used to actively switch the acoustic transmission properties of the hybrid superlattice in a reversible fashion. Moreover, the position and spectral-width of the passing-bands in Figure 3 can be precisely tuned by modulating the power of the laser irradiating the structure. This functionality, which is fully enabled by the unique behavior of photo-elastic chalcogenide glass, indeed can serve purpose in radio frequency signal processing applications such as high-precision filtering.

V. CONCLUSIONS

We have theoretically demonstrated active control over the acoustic properties of a hybrid phononic/photonic superlattice via an application of an external monochromatic light source. The validated technology offers a platform on which more complex radio frequency signal processing functionalities can be constructed. Over the past two decades, the number of wireless technologies

utilizing radio frequencies has increased tremendously. This influx has severely crowded the radio spectrum and, as a consequence, stimulated the need for innovative technologies to facilitate equal-sharing and enhanced access to radio frequency communication. The functions offered by this technology may assist in developing solutions to some of the emerging challenges in radio frequency communications.

[1] M. M. Sigalas and E. N. Economou, "Elastic and acoustic band structure," J. Sound Vib. **158**, 377-382 (1992).
[2] M. Sigalas and E. Economou, "Band structure of elastic waves in two dimensional systems," Solid State Communications **86**, 141 (1993).
[3] M. S. Kushwaha, P. Halevi, L. Dobrzynski, and B. Djafari-Rouhani, "Acoustic band structure of periodic elastic composites," Phys. Rev. Lett. **71**, 2022-2025 (1993).
[4] J. O. Vasseur, P. Deymier, B. Chenni, B. Djafari-Rouhani, L. Dobrzynski, and D. Prevost, "Experimental and theoretical evidence for the existence of absolute acoustic band gaps in two-dimensional solid phononic crystals," Phys. Rev. Lett. **86**(14), 3012–3015 (2001).
[5] S. Yang, J. H. Page, Z. Liu, M. L. Cowan, C. T. Chan, and P. Sheng, "Focusing of sound in a 3D phononic crystal," Phys. Rev. Lett. **93**, 024301 (2004).
[6] J. B. Pendry, "Negative Refraction Makes a Perfect Lens," Phys. Rev. Lett. **85**, 3966 (2000).
[7] M. Ke, Z. Liu, C. Qiu, W. Wang, J. Shi, W. Wen, and P. Sheng, "Negative-refraction imaging with two-dimensional phononic crystals," Phys. Rev. B **72**, 064306 (2005).
[8] A. Sukhovich, L. Jing, and J. H. Page, "Negative refraction and focusing of ultrasound in two-dimensional phononic crystals," Phys. Rev. B **77**, 014301 (2008).
[9] A. Sukhovich, B. Merheb, K. Muralidharan, J. O. Vasseur, Y. Pennec, P. A. Deymier, and J. H. Page, "Experimental and Theoretical Evidence for Subwavelength Imaging in Phononic Crystals," Phys. Rev. Lett. **102**, 154301 (2009).
[10] X. Zhang and Z. Liu, "Negative refraction of acoustic waves in two-dimensional phononic crystals," Appl. Phys. Lett. **85**, 341-343 (2004).
[11] L. Feng, X. Liu, M. Lu, Y. Chen, Y. Chen, Y. Mao, J. Zi, Y. Zhu, S. Zhu, and N. Ming, "Acoustic Backward-Wave Negative Refractions in the Second Band of a Sonic Crystal," Phys. Rev. Lett. **96**, 014301 (2006).
[12] J. Bucay, E. Roussel, J. O. Vasseur, P. A. Deymier, A.-C. Hladky-Hennion, Y. Pennec, K. Muralidharan, B. Djafari-Rouhani, and B. Dubus, "Positive, negative, zero refraction, and beam splitting in a solid/air phononic crystal: Theoretical and experimental study," Phys. Rev. B **79**, 214305 (2009).
[13] N. Swinteck, J.-F. Robillard, S. Bringuier, J. Bucay, K. Muralidaran, J. O. Vasseur, K. Runge, and P. A. Deymier, "Phase-controlling phononic crystal," Appl. Phys. Lett. **98**, 103508 (2011).
[14] N. Swinteck, S. Bringuier, J.-F. Robillard, J.O. Vasseur, A. C. Hladky-Hennion, K. Runge, and P. A. Deymier, "Phase control in two-dimensional phononic crystals," J. Appl. Phys. **110**, 074507 (2011).
[15] D. Richards and D. Pines, "Passive reduction of gear mesh vibration using a periodic drive shaft," Journal of Vibration and Sound **264**, 317342 (2003).
[16] H. Policarpo, M. Neves, and A. Ribeiro, "Dynamical response of a multi-laminated periodic bar: Analytical, numerical and experimental study," Shock and Vibration **17**, 521-535 (2010).
[17] M. Sigalas, "Elastic wave band gaps and defect states in two-dimensional composites," Journal of the Acoustical Society of America **101**(3), 1256-1261 (1997).
[18] M. Torres, F. Montero de Espinosa, D. Garcia-Pablos, and N. Garcia, "Sonic band gaps in finite elastic media: Surface states and localization phenomena in linear and point defects," Physical Review Letters **82**, 3054-3057 (1999).
[19] M. Kafesaki, M. Sigalas, and N. Garcia, "Frequency modulation in the transmittivity of wave guides in elastic-wave band-gap materials," Physical Review Letters **85**, 4044-4047 (2000).
[20] A. Khelif, B. Djafari-Rouhani, J. O. Vasseur, and P. A. Deymier, "Transmission and dispersion relations of perfect and defect-containing waveguide structures in phononic band gap materials," Physical Review B **68**(2), 024302 (2003).
[21] B. Yuan, B. Liang, J. Tao, X. Zou, and J. Cheng, "Broadband directional acoustic waveguide with high efficiency," Applied Physics Letters **101**, 043503 (2012).
[22] L. Chen, C. Kuo, and Z. Ye, "Acoustic imaging and collimating by slabs of sonic crystals madefrom arrays of rigid cylinders in air," Applied Physics Letters **85**, 1072-1074 (2004).
[23] J. Christensen, A. Fernandez-Dominguez, F. de Leon-Perez, L. Martin-Moreno, and F. Garcia-Vida, "Collimation of sound assisted by acoustic surface waves," Nature Physics **3**, 851-852 (2007).
[24] J. Shi, S. Lin, and T. Huang, "Wide-band acoustic collimating by phononic crystal composites," Applied Physics Letters **92**(11), 111901 (2008).
[25] F. Meseguer, M. Holgado, D. Caballero, N. Benaches, J. Sanchez-Dehesa, C. Lopez, and J. Llinares, "Rayleigh-wave attenuation by a semi-infinite two-dimensional elastic-band-gap crystal," Physical Review B **59**(19), 12169-12172 (1999).
[26] R. Sainidou and N. Stefanou, "Guided and quasiguided elastic waves in phononic crystal slabs," Physical Review B **73**, 184301 (2006).
[27] J. Deymier, P. A. Deymier, B. Djafari-Rouhani, Y. Pennec, and A.-C. Hladky-Hennion, "Absolute forbidden bands and waveguiding in two-dimensional phononic crystal plates," Physical Review B **77**, 085415 (2006).
[28] B. Liang, X. Zou, B. Yuan, and J. Cheng, "Frequency-dependence of the acoustic rectifying efficiency of an acoustic diode model," Applied Physics Letters **96**, 233511 (2010).
[29] B. Liang, X. S. Guo, J. Tu, Z. Cheng, and J. C. Cheng, "An acoustic rectifier," Nature Materials **9**, 989-992 (2010).
[30] J.–F. Robillard, O. Bou Matar, J. O. Vasseur, P. A. Deymier, M. Stippinger, A.–C. Hladky-Hennion, Y. Pennec, and B. Djafari-Rouhani, "Tunable magnetoelastic phononic crystals," Applied Physics Letters **95**, 124104 (2009).
[31] O. Bou Matar, J. F. Robillard, J. O. Vasseur, A. C. Hladky-Hennion, P. A. Deymier, P. Pernod, and V. Preobrazhensky, "Band gap tunability of magnetoelastic phononic crystal," Journal of Applied Physics **111**, 054901 (2012).

[32] K. Tanaka and A. Odajima, "Configuration-coordinate model for photodarkening in amorphous As_2S_3," J. Non-Cryst. Sol. **46**, 259-268 (1981).
[33] K. Tanaka, "Photoexpansion in As_2S_3 glass," Phys. Rev. B: Condens. Matter **57**, 5163-5167 (1998).
[34] P. Krecmer, A. M. Moulin, R. J. Stephenson, T. Rayment, M. E. Welland, and S. R. Elliott, "Reversible nanocontraction and dilatation in a solid induced by polarized light," Science **277**, 1799-1802 (1997).
[35] H. Hisakuni and K. Tanaka, "Optical microfabrication of chalcogenide glasses," Science **270**, 974-5 (1995).
[36] J. Gump, I. Finckler, H. Xia, R. Sooryakumar, W. J. Bresser, and P. Boolchand, "Light-induced giant softening of network glasses observed near the mean-field rigidity transition," Phys. Rev. Lett. **92**, 245501 (2004).
[37] A. Feltz, *Amorphous Inorganic Materials and Glasses* (VCH, 1993).
[38] Z. U. Borisova, *Glassy Semiconductors* (Plenum Press, 1981).
[39] E. Walker, D. Reyes, M. M. Rojas, A. Krokhin, Z. Wang, and A. Neogi, "Tunable ultrasonic phononic crystal controlled by infrared radiation," Applied Physics Letters **105**, 143503 (2014).
[40] Y. Ito, S. Kashida, and K. Murase, "Elastic Constants of the Chalcogenide Glasses (Ge_xSe_{1-x}, As_ySe_{1-y} and $Ge_{2/3z}As_{1/3z}Se_{1-z}$)," Solid State Communications **65**(6), 449-452 (1988).
[41] G. Mur, "The Modeling of Singularities in the Finite-Difference Approximation of the Time-Domain electromagnetic-field equations," IEEE Transactions on Microwave Theory and Techniques **EMC-23**, 377 (1981).